iScience

CellPress
OPEN ACCESS

Article

The circadian clock protein Cryptochrome 1 is a direct target and feedback regulator of the Hippo pathway

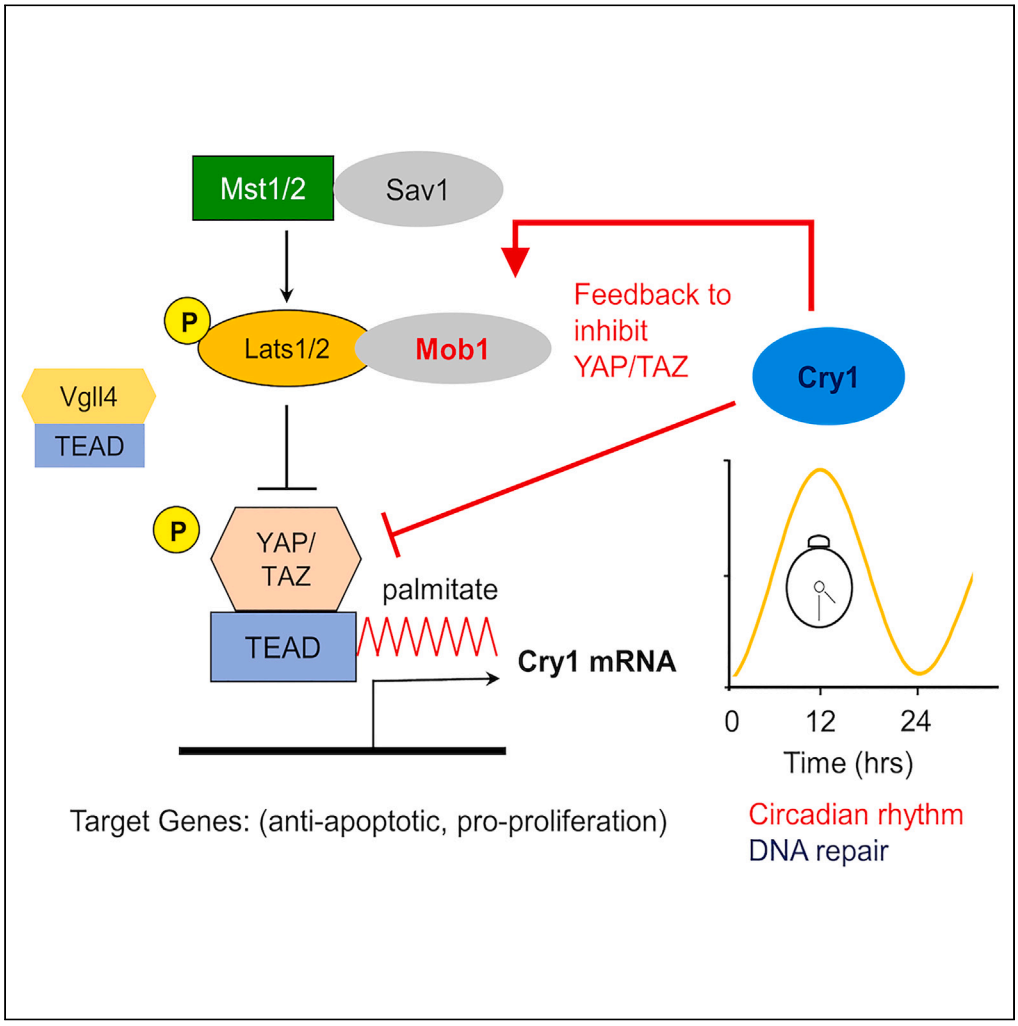

Abdelhalim Azzi, Zhipeng Tao, Yang Sun, Hannah Erb, Carla Guarino, Xu Wu

a.azzi@imol.edu.pl (A.A.)
xwu@cbrc2.mgh.harvard.edu (X.W.)

Highlights

The core clock gene *CRY1* is a direct target gene of TEAD–YAP

YAP silencing or TEAD inhibition leads to decreased *CRY1* expression

CRY1 restricts YAP hyperactivation through regulating MOB1 and YAP expression

Changes in YAP level or activity affects circadian rhythm in synchronized cells

Azzi et al., iScience *26*, 107449
August 18, 2023
https://doi.org/10.1016/j.isci.2023.107449

iScience

CellPress
OPEN ACCESS

Article

The circadian clock protein Cryptochrome 1 is a direct target and feedback regulator of the Hippo pathway

Abdelhalim Azzi,[1,2,*] Zhipeng Tao,[1] Yang Sun,[1] Hannah Erb,[1] Carla Guarino,[1] and Xu Wu[1,3,*]

SUMMARY

Circadian clock controls daily behavior and physiology. The activity of various signaling pathways affects clock gene expression. Here, we show that the core circadian clock gene *CRY1* is a direct target of the Hippo pathway effector YAP. YAP binds to TEADs and occupies the proximal promoter regions of *CRY1*, positively regulating its transcription. Interestingly, we further identified that CRY1 acts in a feedback loop to fine-tune Hippo pathway activation by modulating the expression of *YAP* and *MOB1*. Indeed, loss of CRY1 results in enhanced YAP activation. Consistently, we found that YAP levels and activity control clock gene expression and oscillation in synchronized cells. Furthermore, in breast cancer cells, CRY1 downregulation causes YAP/TAZ hyperactivation and enhanced DNA damage. Together, our findings provide a direct mechanistic link between the Hippo pathway and the circadian clock, where CRY1 and Hippo components form an orchestrated signaling network that influences cell growth and circadian rhythm.

INTRODUCTION

The evolutionarily conserved Hippo pathway controls development, organ size, and regeneration by regulating cell proliferation and survival.[1,2] In mammals, the core Hippo pathway components include the Ste20-like kinase MST1/2 and SAV1 complex, which binds to and phosphorylates the large tumor suppressor 1/2 kinases (LATS1/2) and the scaffolding proteins MOB1A/B. Activation of LATS1/2, in turn, phosphorylates and inactivates the transcriptional co-activators YAP and TAZ (WWTR1). LATS1/2-mediated YAP Ser127 and TAZ Ser89 phosphorylation restrict their nuclear localizations by cytoplasmic sequestration.[2–4] In differentiated cells, YAP and TAZ are usually inactivated by the Hippo pathway to maintain cellular quiescence. However, during development or upon tissue injury, the Hippo pathway could be suppressed, leading to YAP/TAZ activation to promote cellular growth and differentiation, stem cell self-renewal, and tissue repair.[5]

Hippo pathway has been shown to play an important role in tumorigenesis. Indeed, many reports have shown that hyperactivated YAP/TAZ promotes tumor development, metastasis, and therapeutic resistance.[6] For example, amplification of a genomic region containing *YAP* enhances cell proliferation in medulloblastoma.[7] In addition, elevated YAP expression and protein levels have been observed in many cancers, including lung, prostate, ovarian, and liver cancers.[8–11] Although most of the studies support the tumor-promoting function of YAP and TAZ, recent findings have also suggested a tumor suppressive function of YAP in several cancers such as multiple myeloma.[11,12]

YAP and TAZ act as transcriptional coactivators to DNA-binding transcription factors, such as TEAD proteins.[13] These complexes occupy mainly proximal promoter and distal enhancer regions, and regulate the expression of target genes associated with cell growth, survival, and migration.[14] Besides TEAD, YAP/TAZ could interact with other transcription factors, including RUNX2 and SMAD, to regulate expression of different target genes.[15,16] Because of the diversity of the transcriptional output of the Hippo pathway, the nature and the exact function of their target genes in specific tissue and context require detailed characterization. TEAD–YAP complex could regulate transcription of target genes involved in diverse cellular functions,[14] beyond regulation of cell growth, migration, and survival.

[1]Cutaneous Biology Research Center, Massachusetts General Hospital, Harvard Medical School, Charlestown, MA, USA

[2]Present address: IMol Polish Academy of Sciences, Warsaw, Poland.

[3]Lead contact

*Correspondence: a.azzi@imol.edu.pl (A.A.), xwu@cbrc2.mgh.harvard.edu (X.W.)

https://doi.org/10.1016/j.isci.2023.107449

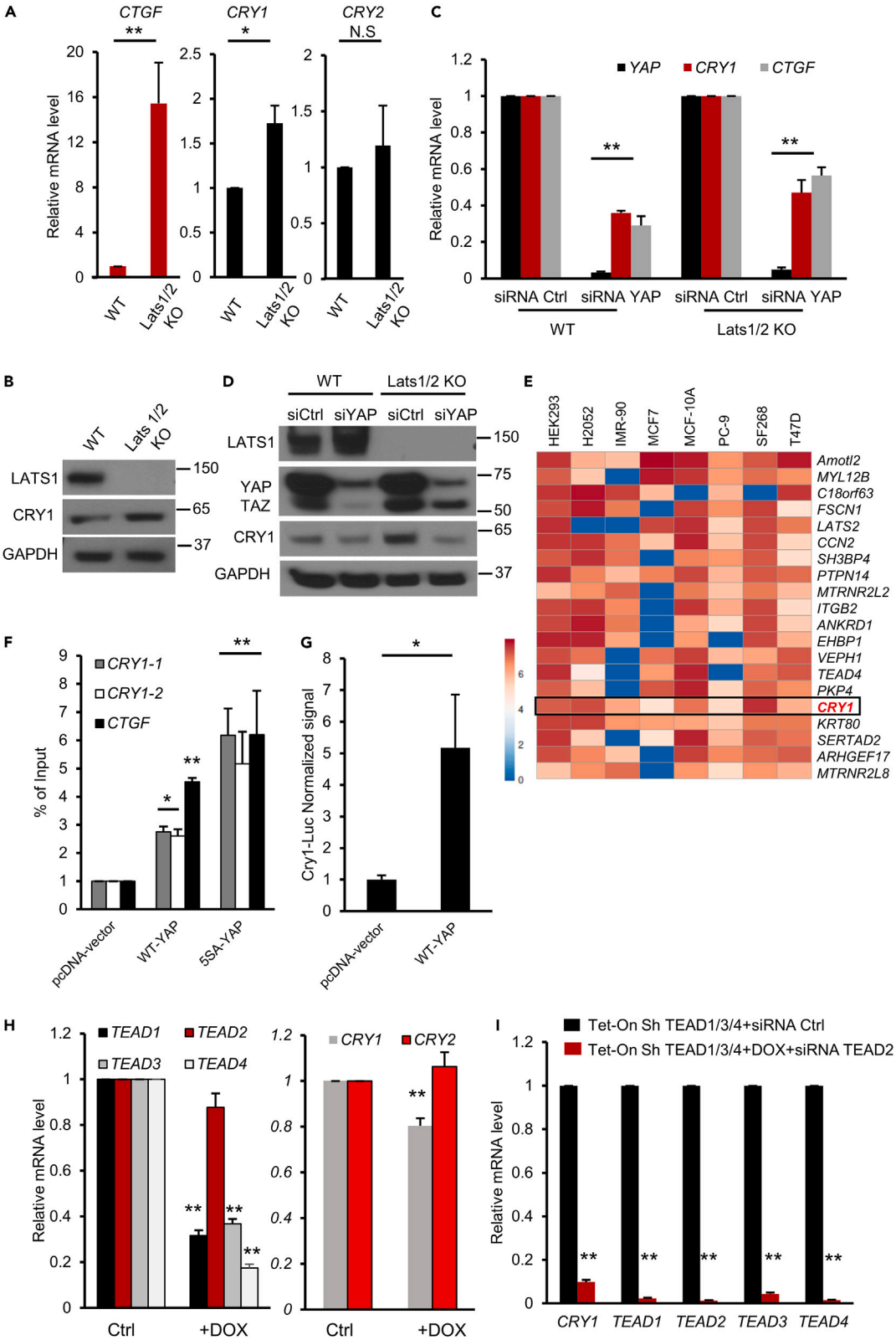
A
CTGF
CRY1
CRY2
N.S
Relative mRNA level
WT
Lats1/2 KO
C
YAP
CRY1
CTGF
Relative mRNA level
siRNA Ctrl
siRNA YAP
WT
Lats1/2 KO
B
WT
Lats 1/2 KO
LATS1
CRY1
GAPDH
D
WT
Lats1/2 KO
siCtrl
siYAP
YAP
TAZ
E
HEK293
H2052
IMR-90
MCF7
MCF-10A
PC-9
SF268
T47D
Amotl2
MYL12B
C18orf63
FSCN1
LATS2
CCN2
SH3BP4
PTPN14
MTRNR2L2
ITGB2
ANKRD1
EHBP1
VEPH1
TEAD4
PKP4
CRY1
KRT80
SERTAD2
ARHGEF17
MTRNR2L8
F
CRY1-1
CRY1-2
CTGF
% of Input
pcDNA-vector
WT-YAP
5SA-YAP
G
Cry1-Luc Normalized signal
pcDNA-vector
WT-YAP
H
TEAD1
TEAD2
TEAD3
TEAD4
CRY1
CRY2
Relative mRNA level
Ctrl
+DOX
I
Tet-On Sh TEAD1/3/4+siRNA Ctrl
Tet-On Sh TEAD1/3/4+DOX+siRNA TEAD2
Relative mRNA level
CRY1
TEAD1
TEAD2
TEAD3
TEAD4

Figure 1. YAP is a direct transcriptional regulator of CRY1

(A) Bar graphs showing mRNA levels of *CTGF*, *CRY1*, and *CRY2* quantified by q-PCR in HEK-293A WT and LATS1/2 knockout cells. n = 3 (biological repeats) for each condition. Values were expressed as mean ± standard error (SEM). Unpaired t-test, *, p<0.05, **, p<0.01.

(B) Lysates from HEK293A cells (WT and LATS1/2 knockout) were separated using SDS-PAGE and blotted with the indicated antibodies.

(C) Downregulation of YAP alters CRY1 RNA and protein levels. Bar graph showing mRNA levels of *YAP*, *CTGF*, and *CRY1* quantified by qPCR in HEK293A WT or LATS 1/2 KO cells transiently transfected with siRNA control or siRNA against YAP. n = 4 (biological repeats) for each condition. Data show means ± SEM, unpaired t-test, **, p<0.01.

(D) Lysate from HEK293A WT and LATS1/2 KO cells transiently transfected with siRNA control (si Ctrl) or siRNA YAP (si YAP).

(E) Heatmap showing direct target genes of YAP from ChIP-seq data retrieved from ChIP-Atlas database.[29] Colors of the cells indicate the normalized MACS2 scores for YAP ChIP-seq peaks within the transcription start site (TSS ±1 kb). Rows indicate the ranked target gene.

(F) Normalized ChIP-qPCR signal in HEK293A transfected with pcDNA-vector control, Flag-YAP (WT) or Flag-YAP (5SA) using Anti-Flag antibody. n = 3 (biological repeats) for each condition. Data are presented as mean ± SEM. CRY1-1 and CRY1-2 are two primer sets close to the TSS (see Figure S1F). One way ANOVA CRY1-1 (F (2, 6) = 22.65, p = 0.0016), CRY1-2(F (2, 6) = 5.424, p = 0.0452), CTGF (F (2, 6) = 15.89, p = 0.004).

(G) Bar graph showing results of Cry1-Luc reporter assay in HEK293A cells transfected with the indicated plasmids. n = 3 (biological repeats) for each condition. Data are the means ± SEM. Unpaired T-test, *, p<0.05.

(H and I) TEAD is required for YAP-induced transcription of CRY1. (H) Bar graph showing mRNA levels of the indicated genes in HEK293A WT cells Tet-On TEAD1/3/4 supplemented or not with 100 ng/ml doxycycline (DOX) during 48h. Data show the change relative to the control. n = 3 (biological repeats) for each condition. Data are the means ± SEM. Unpaired t-test, **, p<0.01. (I) Bar graph showing CRY1, TEAD1/3/4 and TEAD2 mRNA levels in HEK293A cells transfected with siRNA control or siRNA against TEAD2 and supplemented with doxycycline. n = 3 (biological repeats) for each condition. Data show the means ± SEM. Unpaired t-test, **, p<0.01.

The circadian clock is a cell-intrinsic timekeeping system that controls daily variation in several biochemical and physiological processes, including cell growth differentiation, and tissue repair.[17,18] The heterodimer of CLOCK and BMAL1 binds to the promoter regions of clock and clock-controlled genes (CCG), such as *PERIOD* (*PER*) and *CRYPTOCHROME* (*CRY*), enhancing their expression. PER and CRY proteins, in turn, inactivate CLOCK and BMAL1 heterodimers in a feedback regulation.[19,20] This feedback loop controls transcriptional activity and daily variation in transcripts levels of thousands of genes in various tissues and organs, which in turn affect many physiological processes.[21] Circadian homeostasis is required for proper cell growth and differentiation, and alterations in core clock components have been linked to several pathological disorders, including diabetes, neurodegeneration, and cancer.[22] Recently, it has been suggested that Hippo pathway might be involved in the regulation of the circadian clock. For example, YAP-mediated NF-κB activation alters clock gene expression in sarcoma.[23] Moreover, loss of BMAL1 enhances intestinal stem cell self-renewal.[24] Furthermore, Parasram K et al. reported that the circadian clock in intestinal stem cells is positively regulated by the Hippo pathway.[25] However, whether these effects are directly under the control of the Hippo pathway components or their effector proteins remains elusive. To gain mechanistic insights into the Hippo pathway in regulating of cellular circadian genes, we carried out detailed transcriptomic and biochemical studies. Herein, we discovered that the core circadian gene *CRY1* is a direct target of YAP. YAP binds to the proximal promoter region of *CRY1* and positively regulates its transcription in a TEAD-dependent manner. RNAi knockdown and pharmacological inhibition of TEAD–YAP leads to decreased *CRY1* expression and altered circadian oscillation of clock genes. In addition to its role as a core clock component, CRY1 controls expression of genes involved in regulation of DNA replication, DNA damage, and cell cycle.[26,27] Interestingly, we found that CRY1 acts in a feedback loop to limit YAP/TAZ transcription levels and activates the Hippo pathway kinases by regulating MOB1A/B expression. Moreover, we have also shown that downregulation of CRY1 in breast cancer cells leads to hyperactivation of YAP and enhanced DNA-damage responses, which in turn affects cell growth. The combination of a small molecule CRY1 activator and a TEAD inhibitor leads to markedly enhanced anti-proliferative effects. Our work revealed new functions of TEAD–YAP in the direct regulation of cellular circadian genes, an important negative feedback regulation that restricts YAP/TAZ activity, and potential new strategies to enhance the therapeutic activities of TEAD inhibitors.

RESULTS

YAP binds to *CRY1* promoter and regulates its transcription

LATS1/2 kinases act as the major functional regulators of the Hippo pathway. Upon activation, these enzymes directly phosphorylate and inactivate YAP and TAZ,[3,5] which leads to modulation of YAP/TAZ target gene expression. To gain insights into how Hippo pathway effector proteins regulate the expression of clock genes, we first analyzed the impact of YAP activation on clock gene expression levels in HEK293A cells lacking LATS1/2. As expected, the direct YAP target gene *CTGF* expression is markedly elevated in LATS1/2 knockout (KO)[28] cells, as shown in Figure 1A. Interestingly, the loss of LATS1/2 and activation

of YAP lead to a significant increase in CRY1 mRNA and protein levels, whereas the level of CRY2 remain relatively unchanged (Figures 1A and 1B). We next assessed the effect of transient knockdown of YAP in WT and LATS1/2 KO cells. As shown in Figures 1C and 1D, silencing YAP significantly decreases CRY1 mRNA and protein levels in both WT and LATS1/2 KO cells. Consistently, significant changes in transcript levels of *PER2* and *CLOCK* were also seen upon YAP knockdown (Figure S1A). Together, these results show that loss of the Hippo pathway core kinases LATS1/2 could lead to YAP-dependent CRY1 upregulation. In addition to YAP, TAZ (WWTR1) could also regulate *CRY1* transcription. Indeed, overexpression of the WT or the constitutively active TAZ (TAZ-S89A) in HEK293A cells leads to a significant increase in *CRY1* transcript levels (Figures S1B–S1D). Consistently, siRNA knockdown of TAZ leads to a marked decrease in *CRY1* expression levels (Figure S1E), albeit weaker than the effects of YAP. Our results are consistent with previous findings showing that YAP has a more potent effect than TAZ in regulating several target gene expressions.[28]

When associated with DNA-binding transcriptional factors, YAP/TAZ binds to defined genomic regions and regulates target gene transcription. To examine whether YAP localizes and binds to promoter regions of core clock genes, we first used ChIP-Atlas, an online database of the published chromatin immunoprecipitation sequencing (ChIP-seq) data.[29] Interestingly, *CRY1*, a negative regulator of the circadian clock,[19] is among the top YAP target genes in multiple cell lines. Indeed, ChIP-Atlas data showed that YAP binds the region surrounding the transcription start site (TSS) of *CRY1* (TSS is $\pm$1 kb) (Figure 1E). We did not observe strong YAP binding signal for *CRY2* promoter. This observation is consistent with our results, which showed that YAP and TAZ have much stronger effects on *CRY1* transcription when compared to CRY2.

To validate this finding, we examined the occupancy of YAP protein on the promoter region of *CRY1* using chromatin immunoprecipitation (ChIP) and qPCR analysis. Consistently, we observe moderate binding of YAP to *CRY1* promoter in cells transfected with wild-type YAP, while the constitutively active YAP mutant (YAP-5SA) showed a marked increase in ChIP-qPCR signal (Figures 1F and S1F). In line with the ChIP-qPCR results, the activity of a luciferase reporter driven by *CRY1* promoter (pCry1-Luc reporter) was efficiently induced by ectopic expression of YAP (Figure 1G). Taken together, these results show that YAP binds to *CRY1* promoter regions and directly induces its transcription.

TEADs are required for YAP-induced transcription of *CRY1*

YAP and TAZ are transcriptional coactivators, shuttling between the cytoplasm and the nucleus in response to various inputs.[30,31] As they lack DNA-binding properties, their interaction with DNA-binding transcription factors is required for the regulation of target gene expression, and the TEAD family of transcription factors are the major DNA-binding partners of YAP and TAZ.[13,14,32] We used ChIP-seq data available in ChIP-Atlas[29] to visualize TEAD enrichment near the *CRY1* promoter. This bioinformatic approach has shown that *CRY1* is among the top TEAD1 target genes in several cell lines. Indeed, ChIP-Atlas data showed that TEAD1 binds to the region surrounding the transcription start site of *CRY1* (TSS is $\pm$1 kb) (Figure S1G), suggesting a role of TEAD–YAP complex could regulate CRY1 expression. It is worth noting that ChIP-seq data for TEAD2 and TEAD4 are not available in ChIP-Atlas. Therefore, other TEADs might also be involved. We next examined whether TEAD silencing or inhibition could decrease CRY1 RNA and protein levels. As indicated in Figure 1H, the combined silencing of TEAD1/3/4 in HEK293A cells led to a moderate but significant decrease of *CRY1* mRNA levels. Interestingly, additional TEAD2 silencing using siRNA leads to a dramatic decrease in *CRY1* mRNA levels, suggesting a predominant role of this protein in CRY1 regulation when compared to other TEADs (Figure 1I). Indeed, siRNA-mediated knockdown of TEDA2 alone leads to a modest but significant decrease in CRY1 mRNA and protein level (Figure S1H). YAP/TAZ activity could be regulated by cell density-mediated Hippo pathway activation.[30] Therefore, we used low cell density-mediated YAP/TAZ activation and TEAD inhibition to examine CRY1 protein levels. Seeding MCF7 and MDA-MB-231 cells at low density activates YAP, demonstrated by decreased p-YAP (S127) and increased CTGF levels. Consistently, we have observed markedly enhanced CRY1 protein levels. In addition, TEAD inhibition using a small molecule inhibitor (MGH-CP1)[33] abolishes CRY1 upregulation under low density (Figure S1I). Altogether, these data demonstrate that TEAD proteins, particularly TEAD2, are required for YAP-mediated transcriptional regulation of *CRY1*.

CRY1 restricts YAP activation through a negative feedback regulation

In addition to its role as a key component of the core clock machinery, CRY1 has been shown to regulate diverse cellular processes, such as cell growth and DNA repair.[34,35] Therefore, we examined the impact of

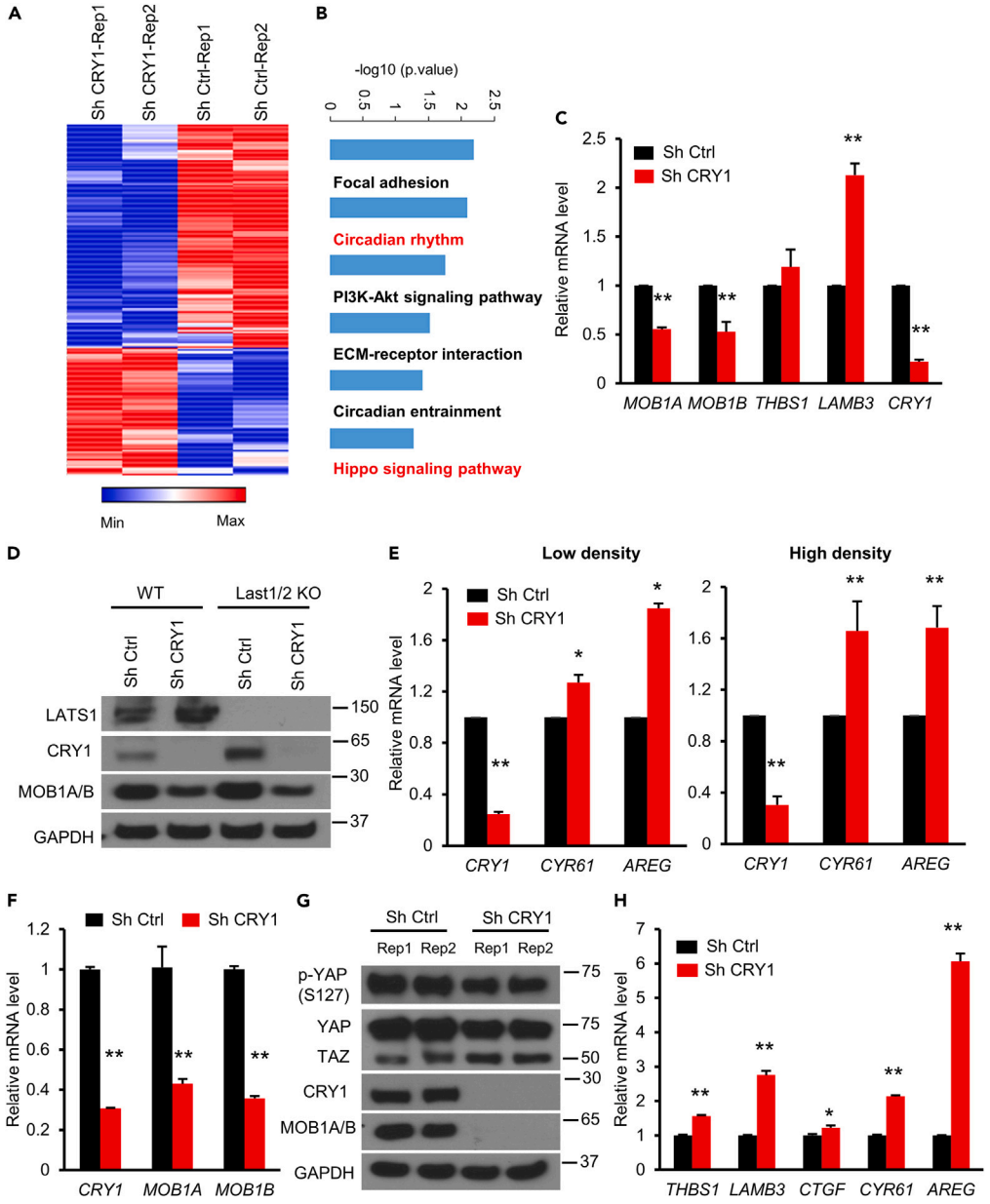

Figure 2. CRY1 knockdown alters Hippo pathway activities and its target genes expression

(A) Heatmap representing color-coded expression levels of differentially expressed genes (DEG) (FDR p.value < 0.05) in wild-type HEK293A cells stably transfected with shRNA control or shRNA against CRY1. Normalized counts were used as input for heatmap generation. Biological replicates in each condition were shown. EdgeR results and DEG are listed in Table S1.

(B) KEGG pathway analysis of the DEG using DAVID Database (Visualization and Integrated Discovery).[36] Results highlight the top affected pathways.

(C) Bar graph showing mRNA levels of candidate genes selected from RNA-seq data. mRNA quantified by qPCR in HEK293A WT cells stably transfected with shRNA control or shRNA against CRY1. Data show the means ± SEM. Unpaired t-test, **, p<0.01.

(D) Immunoblot results of the protein lysate from HEK293A WT and LATS 1/2 KO cells stably transfected with shRNA control or shRNA against CRY1 stained for the indicated antibodies.

(E) Bar graphs showing mRNA levels of the indicated genes in HEK293A stably expressing shRNA control or shRNA against CRY1 seeded at high or low density. Data display the change relative to the shRNA control cells. Data show the means ± SEM. Unpaired t-test, *, p<0.05, **, p<0.01.

Figure 2. *Continued*

(F) Bar graph indicating mRNA levels of the specified genes quantified by qPCR in MDA-MB-231 cells stably transfected with shRNA control or shRNA against CRY1. Results were standardized relative to shRNA control. Data are the means ± SEM from three independent experiments. Unpaired t-test, **, p<0.01.

(G) Lysate from MDA-MB-231 cells stably transfected with shRNA control or shRNA against CRY1 were immunoblotted with the indicated antibodies.

(H) Bar graph showing mRNA levels of the YAP/TAZ target genes analyzed as in MDA-MB-231 as in F. Data are the means ± SEM from three independent experiments. Unpaired t-test, *, p<0.05, **, p<0.01.

its knockdown on global transcription in HEK293A cells using RNA-seq (GSE216975). Stable silencing of CRY1 with short hairpin RNA in HEK293A cells was successfully established and validated by qRT-PCR and Western blot. As shown in Figure 2A, CRY1 knockdown significantly alters the expression level of 237 genes, of which 151 downregulated and 86 upregulated in CRY1 depleted cells relative to shRNA control (FDR p value <0.05). Functional analysis, using Database for Annotation, Visualization and Integrated Discovery (DAVID),[36] showed that genes altered upon CRY1 depletion regulate several processes, including circadian rhythm. Interestingly, in addition to circadian rhythm, the PI3K pathway and Hippo pathway are also among the top signaling pathways affected (Figure 2B). In addition, Gene Set Enrichment Analysis (GSEA)[37] showed that both the PI3K and Hippo signaling pathways are altered following CRY1 knockdown, further confirming a possible cross-regulation between CRY1 protein and these signaling pathways (Figure S2A). Among the candidate genes associated with the Hippo pathway, *Mob1a* and *Mob1b*, *Lamb3* and *Thbs1* are significantly affected upon CRY1 downregulation (Table S1).

We next selected several candidate genes from RNA-seq analysis for independent validation by qRT-PCR upon stable knockdown of CRY1. As shown in Figure 2C, the changes in the expression of the selected target genes are consistent with the RNA-seq data. MOB1A/B are adaptor proteins that bind to and enhance the kinase activity of LATS1/2 proteins,[38] leading to YAP/TAZ phosphorylation and inhibition, and *Thbs1* and *Lamb3* are direct transcriptional targets of YAP.[29,39] Consistently, CRY1 depletion leads to marked decrease in MOB1A/B protein levels in HEK293A WT and LATS1/2 KO cells (Figure 2D). Furthermore, transient knockdown of CRY1 using a different shRNA, which has weaker knockdown efficiency, leads to a significant decrease in *MOB1B* transcript levels (Figure S2B). We next analyzed how stable CRY1 depletion impacts YAP/TAZ target's gene expression under different conditions. As indicated in Figure 2E, in CRY1 depleted cells, YAP transcriptional activity is higher regardless of cell density. In addition, expression levels of YAP target genes are significantly elevated in CRY1-knockdown cells seeded at high density, suggesting that loss of CRY1 could rescue Hippo pathway-mediated YAP inhibition. In contrary to cell density effects, CRY1 depletion leads to only moderate changes in transcript levels of YAP target genes upon serum stimulation (Figure S2C), suggesting a stimuli-dependent effect of CRY1 on YAP activity.

Dysregulation of Hippo pathway and activation of YAP/TAZ has been reported to occur in several cancers.[8–10] Using the GEPIA platform, containing RNA-seq expression data of tumors and normal samples from the Cancer Genome Atlas (TCGA) and the Genotype-Tissue Expression (GTEx) projects,[40] we examined the correlation between *YAP* and *CRY1* transcript levels. When performed in all cancers, significant positive correlation has been observed between YAP and CRY1 with Spearman correlation R = 0.36 (Figure S2D). In agreement with previous findings that reported overactivation of YAP in a subset of breast cancer,[41] significant positive correlation between *YAP* and *CRY1* RNA levels is also seen in breast cancer samples (Spearman correlation R = 0.5, p = 1.32335E-35) (Figure S2E), further validating our findings related to direct regulation of CRY1 by YAP. In line with these correlations and the results obtained in HEK293A cells, stable CRY1 knockdown in breast cancer cell line MDA-MB-231 leads to a dramatic decrease in transcript and protein levels of the Hippo pathway adaptor protein MOB1A/B (Figures 2F and 2G). Consistent with the function of MOB1A/B as negative regulator of YAP/TAZ activities,[38] YAP/TAZ transcriptional activity is markedly higher in CRY1-knockdown cells, as demonstrated by a significant increase in transcript levels of their direct target genes (Figure 2H). Furthermore, YAP phosphorylation (Ser127) displays lower levels in CRY1-depleted cells, consistent with the known functions of MOB1A/B as a regulator of Hippo pathway (Figure 2G). Together, these data suggest that CRY1 knockdown leads to decreased MOB1A/B levels, which in turn enhance YAP/TAZ transcriptional activities.

CRY1 attenuates transcription of the Hippo pathway effectors YAP and TAZ

Besides its role in the maintenance of the circadian feedback loop, CRY1 is also known as a transcriptional repressor, regulating several processes such as DNA damage response,[34,35] glucocorticoid signaling,[42]

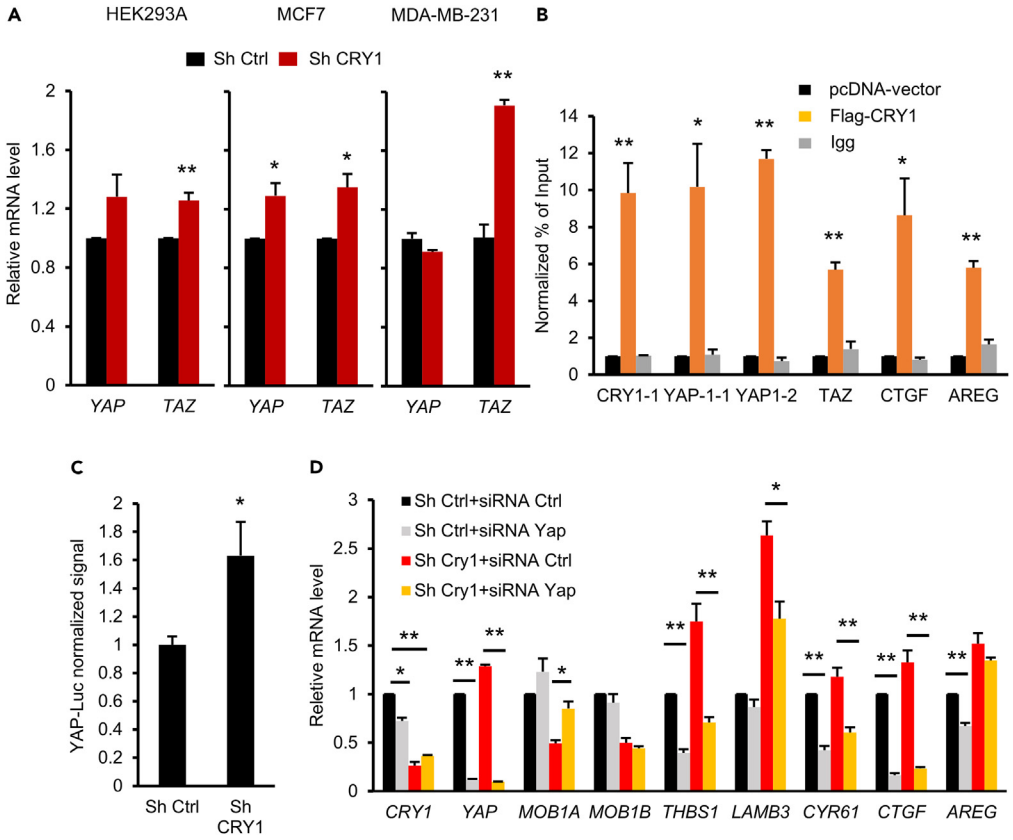

Figure 3. CRY1 regulates transcription of the Hippo pathway effectors YAP and TAZ

(A) Bar graphs showing mRNA levels of *YAP* and *TAZ* in HEK293A, MCF-7 and MDA-MB-231 cells stably transfected with shRNA control or shRNA against CRY1. Unpaired T test, *, p<0.05, **, p<0.01.

(B) Normalized ChIP-qPCR results in HEK293A WT transfected with pcDNA-vector or Flag-CRY1 using Anti-Flag antibody. n = 3 (biological repeats) for each condition. Data are presented as mean ± SEM. YAP1-1 and YAP1-2 are two primer sets that are close to the TSS. Unpaired t-test, *, p<0.05, **, p<0.01. Quantification is normalized to pcDNA-vector control (see Figure S3B). Chromatin from cells transfected with Flag-CRY1 immunoprecipitated with Igg used as a negative control.

(C) Bar graph showing results of YAP-Luc reporter assay in HEK293A cells stably expressing shRNA control or shRNA against CRY1. Data are the means ± SEM. Unpaired t-test, *, p<0.05.

(D) Bar graph showing the effect of transient YAP depletion on transcript level of the indicated genes inHEK293A WT cells stably transfected with shRNA Ctrl or shRNA CRY1. Unpaired t-test, *, p<0.05, **, p<0.01, only statistics for siRNA control vs. siRNA YAP of each genotype were shown. Data are the means ± SEM from three independent experiments.

and glucose metabolism.[43] *YAP* and *TAZ* mRNA levels display a moderate increase in HEK293A cells following CRY1 knockdown, with TAZ transcription showing more significant increase (Figure 3A), suggesting that CRY1 might attenuate YAP/TAZ transcription. Interestingly, these changes were also observed in breast cancer cell lines MCF7 and MDA-MB-231, in which CRY1 knockdown leads to a significant increase of both *YAP* and *TAZ* transcript levels in MCF7 cells, and induces TAZ expression more significantly in MDA-MB-231 cells. These results suggest that CRY1 might regulate YAP and TAZ expressions, but with variable responses in different cell lines (Figure 3A). Consistently, analysis of published expression array data from mouse embryonic fibroblasts lacking *Cry1/2* genes[42] showed a significant increase in both *Yap* and *Taz* transcripts, as well as their direct target genes (*Ctgf*, *Cyr61*, and *Thbs1*) (Figure S3A). To test whether CRY1 could directly bind to YAP and TAZ promoters and regulate their transcription, we performed ChIP-qPCR assays in HEK293A cells following transfection with vector control or Flag-tagged human CRY1. CRY1 protein is markedly enriched in the region surrounding CRY1 promoter (Figures 3B and S3B), consistent with the circadian regulatory mechanisms in which CRY1 positively regulates its own expression when in complex with Bmal1 and Clock.[44] Interestingly, we also observed a significant enrichment of CRY1 in the selected regions of *YAP* promoter. Even though at a moderate level, CRY1 protein is also enriched in *TAZ*, *CTGF* and *AREG* promoter regions (Figure 3B). Consistently, analysis of the previously

published ChIP-seq data from mouse livers revealed that Cry1 binds to the promoter regions of *Yap*, *Areg*, *Lamb3*, and *Cyr61* in a time-of-day dependent manner[21] (Figures S3C–S3E). To further establish the transcriptional control of CRY1 on the YAP promoter, we performed luciferase reporter assays. A sequence encompassing the promoter region of YAP was cloned into pEZX-PG02 basic vector to drive the expression of a firefly luciferase gene. This experiment revealed that CRY1 could suppress YAP expression. Indeed, consistent with transcriptional changes, YAP promoter reporter activity displays a significant increase in cells with CRY1 silencing (Figure 3C). Altogether, these findings show that CRY1 is able to modulate YAP transcription directly. To further examine the impact of YAP overactivation following CRY1 knockdown, we assessed the impact of its transient knockdown in cells expressing empty vector or CRY1 shRNA. While only moderate changes were seen in non-YAP target genes such as *Mob1b*, we observe that YAP knockdown could rescue the induction of its target genes upon CRY1 knockdown, demonstrating that the CRY1-loss mediated target gene induction is due to overactivation of YAP (Figure 3D). Taken together, these findings demonstrate that both YAP and CRY1 exert an effect on each other, suggesting a transcriptional feedback loop between them. However, YAP exerts a stronger effect than CRY1. Indeed, overexpression of CRY1 had only a moderate effect on YAP/TAZ levels (Figures S3F and S3G), while YAP knockdown could rescue almost all of the activity from CRY1.

YAP and TAZ regulate the oscillation of clock genes in cultured cells

Our results demonstrate that YAP directly regulates *CRY1* transcription. Moreover, alteration in other clock genes, such as *PER2* and *CLOCK* were also observed upon YAP knockdown (Figure S1A). To gain insights into how YAP affects the oscillation of clock genes, we analyzed the expression of clock genes upon ectopic expression of YAP. MCF10A cells stably expressing empty vector, wild type (WT), or constitutive active YAP (YAP S127A) were synchronized with dexamethasone, and RNA samples were then collected at the indicated time points (Figure 4A). Overexpression of WT YAP has moderate but significant effects on transcript levels and oscillations of *CRY1*, *CRY2*, *BMAL1* and *PER2*. Interestingly, cells expressing constitutively active YAP (YAP S127A) display marked alterations in both the intensity and oscillation of these clock genes. Indeed, while *PER2* oscillation was completely abolished, we noticed a dramatic increase in CRY1 RNA and protein levels throughout the circadian cycle (Figures 4A and S4A). These data demonstrate that constitutive activation of YAP alters levels and rhythmic oscillation of clock genes.

We tested the rhythmic oscillation of YAP/TAZ and their target genes in U2OS cells, a common cellular model system for monitoring circadian rhythm *in vitro*. Consistent with the data shown in MCF10A cells (Figure 4A), *YAP* and *TAZ* transcripts and their target genes display stable levels throughout the circadian cycle *in vitro* (Figures S4B–S4D). Next, to determine whether alteration in YAP and TAZ expression could disrupt the cellular clock machinery, we have established stable knockdown of YAP or TAZ using shRNAs in U2OS cells. Following dexamethasone synchronization, gene expression in shRNA control and YAP/TAZ knockdown cells were measured. Antiphase oscillation of *PER2* and *BMAL1* RNAs were clearly observed in control cells, indicating successful clock synchronization. Interestingly, YAP or TAZ knockdown profoundly alters the rhythmic transcription of these genes. Consistently, YAP or TAZ knockdown leads to markedly lower *CRY1* transcription (Figure 4B). Moreover, our data show that YAP/TAZ knockdown also alters other clock genes. For example, decreases in *CRY2* expression and *PER2* oscillations were also observed, indicating alteration in both transcriptional levels and circadian oscillation of clock genes in cells (Figure 4B). Although these genes are not direct targets of the Hippo pathway, the alternation might be resulted in disruption of the core circadian rhythm through altered CRY1 expression. Independently, dexamethasone synchronization following transient knockdown of YAP or TAZ by siRNA also leads to a dramatic decrease in CRY1 protein levels throughout the circadian cycle, consistent with the results with shRNAs (Figures S4F and S4G). Furthermore, dampening in *PER2* oscillation and decrease in *CRY1*/2 transcript levels were also seen when cells with stable YAP and TAZ depletion were seeded at low density (Figures S4H–S4M). Consistently, circadian variation in both *CRY1* protein and RNA levels, and the expression of *BMAL1* and *PER2* were markedly altered in cells treated with TEAD inhibitor (Figures S5A–S5D). Taken together, these findings demonstrate that genetic or pharmacological inhibition of the Hippo pathway transcriptional complex TEAD-YAP alters both intensity and rhythmic oscillations of clock gene expression.

DISCUSSION

The Hippo pathway plays a critical role in cell proliferation, survival, and organ size control in development. Several recent reports have shown that hyperactivation of YAP and TAZ is critical in cancer development and progression. Similarly, dysregulation of the circadian clock has also been linked to tumorigenesis.

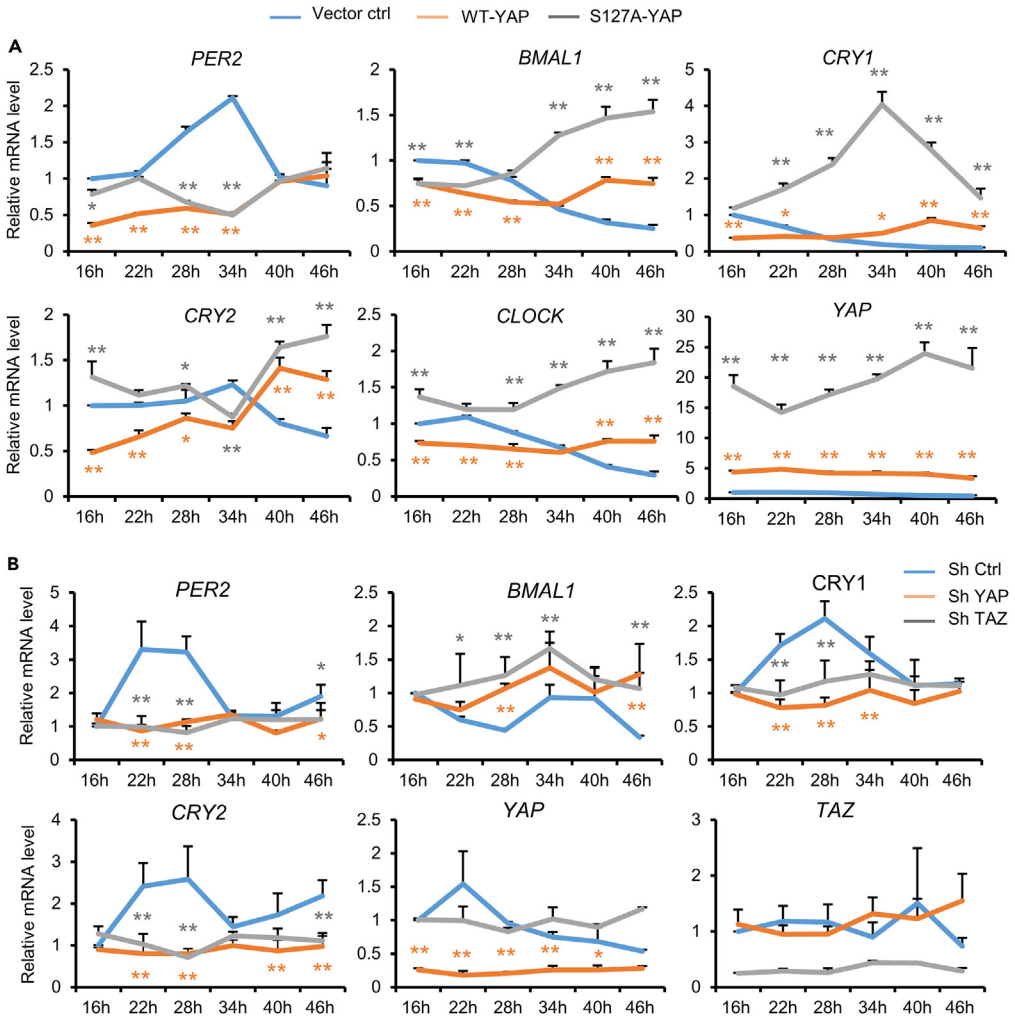

Figure 4. YAP and TAZ downregulation disrupts circadian rhythm

(A) Circadian variation of clock gene expression in MCF10A cells with WT-YAP, YAP-S127A, or control vector (p-Babe) stable overexpression. Cells were synchronized with dexamethasone then collected at the indicated times. Data are the means ± SEM from three independent experiments. Tow-way ANOVA PER2 ($F(10, 36) = 53.69$, $p < 0.0001$)), BMAL1 ($F(10, 36) = 129.6$, $p < 0.0001$)), CRY1 ($F(10, 36) = 93.1$, $p < 0.0001$)), CRY2 ($F(10, 36) = 46.79$, $p < 0.0001$)), CLOCK ($F(10, 36) = 46.98$, $p < 0.0001$)), YAP ($F(10, 36) = 11.34$, $p < 0.0001$)). Dunnett's multiple comparisons tests, *, $p<0.05$, **, $p<0.01$. Detailed statistical analysis and results are shown in Table S4.

(B) U2OS cells stably expressing empty vector (*p*-LKO), shRNA YAP, or shRNA TAZ synchronized with dexamethasone then collected at the indicated times. RNA levels of the indicated genes were measured using q-PCR. Data are the means ± SEM from three independent experiments. Tow-way ANOVA PER2 ($F(10, 36) = 12.21$, $p < 0.0001$)), BMAL1 ($F(10, 36) = 2.383$, $p = 0.0276$)), CRY1 ($F(10, 36) = 5.762$, $p < 0.0001$)), CRY2 ($F(10, 36) = 5.447$, $p < 0.0001$)), YAP ($F(5, 24) = 8.887$, $p < 0.0001$)). Dunnett's multiple comparisons tests, *, $p<0.05$, **, $p<0.01$. Detailed statistical analysis and results are shown in Table S4.

Although a possible link between the Hippo pathway and the circadian clock has been suggested,[23,25] the mechanistic insights underlying the crosstalk remain unknown.

Interrogating genome-wide YAP binding sites using ChIP-Atlas,[29] we found that the promoter region of the negative regulator of the circadian feedback loop, *Cryptochrome 1*, is among the top enriched binding sites of YAP. In addition, CRY1 plays an important feedback regulatory role in fine-tuning Hippo pathway activities, leading to restriction of YAP hyperactivation. Our work provided a detailed mechanistic view of the delicate and highly orchestrated crosstalk between circadian rhythm and the Hippo pathway. Disruption of this delicate balance would lead to hyperactivation of YAP. Interestingly, pharmacological inhibitors

of TEAD also alter CRY1 transcription, which could disrupt the feedback regulation. Consistent with this notion, we found that the combination of a TEAD inhibitor (MGH-CP1) with a CRY1 activator (KL001) exhibits strong synergy in inhibiting YAP-dependent cancer cell proliferation (Figure S5H). Several TEAD inhibitors have been developed, and are currently in clinical studies for YAP-dependent cancers. It would be interesting to see whether TEAD inhibitors could alter the circadian rhythm in humans, and whether changes in CRY1 activity could affect the therapeutic efficacy.

Interestingly, our data also suggest that YAP exert a stronger effect on this feedback loop over CRY1. Indeed, while we observe strong enrichment of CRY1 near the promoter region of YAP and TAZ, overexpression of CRY1 leads to only moderate changes in YAP/TAZ expression levels. Two possibilities might explain this differential effect. First, the binding of CRY1 to YAP promoter may occur in time-of-day dependent manner. Indeed, CRY1 chromatin binding data *in vivo* corroborate with this hypothesis (Figures S3C–S3F) and suggest that CRY1 might exert its negative effect on YAP in tissue specific and time-of-day dependent manner. The second possibility is that CRY1 does not fully inhibit YAP/TAZ transcriptional activities, but prevents their "over-activation". Indeed, studies have shown that overactivation of YAP triggers hyper-transcription accompanied by an increase in DNA damage.[45] Besides its role in the circadian clock, CRY1 is also involved in several other processes, including DNA repair and cell cycle progression.[26,34,35] Indeed, DNA damage responses induce CRY1 stabilization, which promotes DNA repair and cell survival.[35] Consistently, our results demonstrated that CRY1 depletion in breast cancer cells enhances DNA damage responses and alters cell growth (Figures S5E–S5G), which could be through YAP-dependent or -independent mechanisms. Although it is widely accepted that overactivation of YAP and TAZ positively contribute to cell growth, this dogma is challenged by recent observations that hyperactivation of YAP may also have a tumor-suppressing function. For example, hyperactivation of YAP/TAZ renders cancer cells sensitivity to oxidative stress and ferroptosis.[46] In addition, YAP has been shown to bind to p73 to mediate apoptosis under DNA damage.[47] Therefore, it is possible to speculate that YAP-induced CRY1 expression might play an important role in preventing YAP overactivation and cell death and enhances DNA repair and cell proliferation, thereby providing a growth advantage in cancers with deregulated Hippo pathway. Future studies with more comprehensive investigations would be needed to validate these possibilities.

The crosstalk between the Hippo pathway and the circadian clock seems to be evolutionarily conserved. In fact, a recent study showed that overexpression of Yorkie in *Drosophila* enhances CLK/CYC activity.[25] In addition, Rivera-Reyes et al. showed that the downregulation of YAP enhances expression of CRY2 and Bmal1.[23] These findings were observed in a mouse model of undifferentiated pleomorphic sarcoma[23] that lacks p53 and harbors the mutant KRAS,[48] which might contribute to the differential regulation of clock genes by YAP.

Our results showed that YAP has a much stronger effect on CRY1 transcriptional regulation when compared to TAZ. Although YAP and TAZ were often considered as functionally redundant, they do exhibit differences in transcriptional activities.[28] Given the divergence in expression levels of these factors in different tissues, YAP and TAZ may contribute differently to circadian homeostasis in various organs and tissues during development. In addition, YAP/TAZ and clock genes have been associated with tumor growth and metastasis. Therefore, further exploration of the crosstalk between the two pathways will likely shed light on how circadian rhythm is involved in tumorigenesis, potentially providing new therapeutic opportunities for cancers.

Limitations of the study

In summary, Hippo pathway effector YAP plays a key role in regulation of clock gene expression and oscillation in synchronized cells. However, our work was limited to the *in vitro* system. Indeed, given the impact that the circadian clock exerts on behavior and physiology, it would be of great interest to address the impact of Hippo pathway dysregulation on the temporal variation in physiology using an *in vivo* system. Moreover, our data show that CRY1 depletion enhances DNA damage in cancer cells. Whether this effect is directly linked to changes in YAP or Hippo pathway activity is currently unknown. Both components of the Hippo pathway and the circadian clock play an important role in genomic integrity. Therefore, further studies are needed to clarify the exact link between these components in the maintenance of genomic integrity in normal and transformed cells.

STAR★METHODS

Detailed methods are provided in the online version of this paper and include the following:

- KEY RESOURCES TABLE
- RESOURCE AVAILABILITY
  - Lead contact
  - Materials availability
  - Data and code availability
- EXPERIMENTAL MODEL AND STUDY PARTICIPANT DETAILS
  - Cell culture
- METHOD DETAILS
  - Quantitative real-time PCR
  - Transient transfection
  - Packaging shRNA-Encoding Lentivirus
  - Lentivirus infection and selection
  - Western blotting
  - RNA-seq data analysis
  - Colony forming assay
  - Chromatin immunoprecipitation assay
  - Luciferase reporter assay
- QUANTIFICATION AND STATISTICAL ANALYSIS

SUPPLEMENTAL INFORMATION

Supplemental information can be found online at https://doi.org/10.1016/j.isci.2023.107449.

ACKNOWLEDGMENTS

We thank NIH fundings (R01CA219814 and R01CA238270 to X.W.) for support of the work. C.G. was supported by a postdoc fellowship from American-Italian Cancer Foundation. Z.T. was supported partly by a postdoc fellowship from Melanoma Research Alliance. Lats1/2 KO HEK293 cell line is a gift from Dr. W. Wang (UCI).

AUTHOR CONTRIBUTIONS

A.A., Y.S., and X.W. designed the research; A.A., Y.S., Z.T., C.G., and E.H. performed the experimental work; A.A., Y.S., Z.T., and X.W. analyzed the data; A.A., Z.T., and X.W. wrote the manuscript.

DECLARATION OF INTERESTS

X.W. has a financial interest in Tasca Therapeutics, which is developing small molecule modulators of TEAD palmitoylation and transcription factors. X.W.'s interests were reviewed and are managed by Mass General Hospital, and Mass General Brigham in accordance with their conflict of interest policies.

Received: March 2, 2023
Revised: June 19, 2023
Accepted: July 17, 2023
Published: July 20, 2023

REFERENCES

1. Camargo, F.D., Gokhale, S., Johnnidis, J.B., Fu, D., Bell, G.W., Jaenisch, R., and Brummelkamp, T.R. (2007). YAP1 increases organ size and expands undifferentiated progenitor cells. Curr. Biol. *17*, 2054–2060. https://doi.org/10.1016/j.cub.2007.10.039.

2. Dong, J., Feldmann, G., Huang, J., Wu, S., Zhang, N., Comerford, S.A., Gayyed, M.F., Anders, R.A., Maitra, A., and Pan, D. (2007). Elucidation of a universal size-control mechanism in Drosophila and mammals. Cell *130*, 1120–1133. https://doi.org/10.1016/j.cell.2007.07.019.

3. Furth, N., and Aylon, Y. (2017). The LATS1 and LATS2 tumor suppressors: beyond the Hippo pathway. Cell Death Differ. *24*, 1488–1501. https://doi.org/10.1038/cdd.2017.99.

4. Huang, J., Wu, S., Barrera, J., Matthews, K., and Pan, D. (2005). The Hippo signaling pathway coordinately regulates cell proliferation and apoptosis by inactivating Yorkie, the Drosophila Homolog of YAP. Cell *122*, 421–434. https://doi.org/10.1016/j.cell.2005.06.007.

5. Ma, S., Meng, Z., Chen, R., and Guan, K.L. (2019). The Hippo pathway: biology and pathophysiology. Annu. Rev. Biochem. *88*, 577–604. https://doi.org/10.1146/annurev-biochem-013118-111829.

6. Nguyen, C.D.K., and Yi, C. (2019). YAP/TAZ signaling and resistance to cancer therapy. Trends Cancer *5*, 283–296. https://doi.org/10.1016/j.trecan.2019.02.010.

7. Fernandez-L, A., Northcott, P.A., Dalton, J., Fraga, C., Ellison, D., Angers, S., Taylor, M.D., and Kenney, A.M. (2009). YAP1 is amplified and up-regulated in hedgehog-associated medulloblastomas and mediates Sonic hedgehog-driven neural precursor proliferation. Genes Dev. *23*, 2729–2741. https://doi.org/10.1101/gad.1824509.

8. Overholtzer, M., Zhang, J., Smolen, G.A., Muir, B., Li, W., Sgroi, D.C., Deng, C.X., Brugge, J.S., and Haber, D.A. (2006). Transforming properties of YAP, a candidate oncogene on the chromosome 11q22 amplicon. Proc. Natl. Acad. Sci. USA *103*, 12405–12410. https://doi.org/10.1073/pnas.0605579103.

9. Xu, M.Z., Yao, T.J., Lee, N.P.Y., Ng, I.O.L., Chan, Y.T., Zender, L., Lowe, S.W., Poon, R.T.P., and Luk, J.M. (2009). Yes-associated protein is an independent prognostic marker in hepatocellular carcinoma. Cancer *115*, 4576–4585. https://doi.org/10.1002/cncr.24495.

10. Zhao, W., Wang, M., Cai, M., Zhang, C., Qiu, Y., Wang, X., Zhang, T., Zhou, H., Wang, J., Zhao, W., and Shao, R. (2021). Transcriptional co-activators YAP/TAZ: Potential therapeutic targets for metastatic breast cancer. Biomed. Pharmacother. *133*, 110956. https://doi.org/10.1016/j.biopha.2020.110956.

11. Huang, H., Zhang, W., Pan, Y., Gao, Y., Deng, L., Li, F., Li, F., Ma, X., Hou, S., Xu, J., et al. (2017). YAP suppresses lung squamous cell carcinoma progression via deregulation of the DNp63-GPX2 axis and ROS accumulation. Cancer Res. *77*, 5769–5781. https://doi.org/10.1158/0008-5472.CAN-17-0449.

12. Cottini, F., Hideshima, T., Xu, C., Sattler, M., Dori, M., Agnelli, L., ten Hacken, E., Bertilaccio, M.T., Antonini, E., Neri, A., et al. (2014). Rescue of Hippo coactivator YAP1 triggers DNA damage-induced apoptosis in hematological cancers. Nat. Med. *20*, 599–606. https://doi.org/10.1038/nm.3562.

13. Vassilev, A., Kaneko, K.J., Shu, H., Zhao, Y., and DePamphilis, M.L. (2001). TEAD/TEF transcription factors utilize the activation domain of YAP65, a Src/Yes-associated protein localized in the cytoplasm. Genes Dev. *15*, 1229–1241. https://doi.org/10.1101/gad.888601.

14. Zanconato, F., Forcato, M., Battilana, G., Azzolin, L., Quaranta, E., Bodega, B., Rosato, A., Bicciato, S., Cordenonsi, M., and Piccolo, S. (2015). Genome-wide association between YAP/TAZ/TEAD and AP-1 at enhancers drives oncogenic growth. Nat. Cell Biol. *17*, 1218–1227. https://doi.org/10.1038/ncb3216.

15. Zaidi, S.K., Sullivan, A.J., Medina, R., Ito, Y., van Wijnen, A.J., Stein, J.L., Lian, J.B., and Stein, G.S. (2004). Tyrosine phosphorylation controls Runx2-mediated subnuclear targeting of YAP to repress transcription. EMBO J. *23*, 790–799. https://doi.org/10.1038/sj.emboj.7600073.

16. Fujii, M., Nakanishi, H., Toyoda, T., Tanaka, I., Kondo, Y., Osada, H., and Sekido, Y. (2012). Convergent signaling in the regulation of connective tissue growth factor in malignant mesothelioma: TGFβ signaling and defects in the Hippo signaling cascade. Cell Cycle *11*, 3373–3379. https://doi.org/10.4161/cc.21397.

17. Bieler, J., Cannavo, R., Gustafson, K., Gobet, C., Gatfield, D., and Naef, F. (2014). Robust synchronization of coupled circadian and cell cycle oscillators in single mammalian cells. Mol. Syst. Biol. *10*, 739. https://doi.org/10.15252/msb.20145218.

18. Zhang, Z.B., Sinha, J., Bahrami-Nejad, Z., and Teruel, M.N. (2022). The circadian clock mediates daily bursts of cell differentiation by periodically restricting cell-differentiation commitment. Proc. Natl. Acad. Sci. USA *119*, e2204470119. https://doi.org/10.1073/pnas.2204470119.

19. Patke, A., Young, M.W., and Axelrod, S. (2020). Molecular mechanisms and physiological importance of circadian rhythms. Nat. Rev. Mol. Cell Biol. *21*, 67–84. https://doi.org/10.1038/s41580-019-0179-2.

20. Brown, S.A., Kowalska, E., and Dallmann, R. (2012). (Re)inventing the circadian feedback loop. Dev. Cell *22*, 477–487. https://doi.org/10.1016/j.devcel.2012.02.007.

21. Koike, N., Yoo, S.H., Huang, H.C., Kumar, V., Lee, C., Kim, T.K., and Takahashi, J.S. (2012). Transcriptional architecture and chromatin landscape of the core circadian clock in mammals. Science *338*, 349–354. https://doi.org/10.1126/science.1226339.

22. Roenneberg, T., and Merrow, M. (2016). The circadian clock and human health. Curr. Biol. *26*, R432–R443. https://doi.org/10.1016/j.cub.2016.04.011.

23. Rivera-Reyes, A., Ye, S., E Marino, G., Egolf, S., E Ciotti, G., Chor, S., Liu, Y., Posimo, J.M., Park, P.M.C., Pak, K., et al. (2018). YAP1 enhances NF-κB-dependent and independent effects on clock-mediated unfolded protein responses and autophagy in sarcoma. Cell Death Dis. *9*, 1108. https://doi.org/10.1038/s41419-018-1142-4.

24. Stokes, K., Nunes, M., Trombley, C., Flôres, D.E.F.L., Wu, G., Taleb, Z., Alkhateeb, A., Banskota, S., Harris, C., Love, O.P., et al. (2021). The circadian clock gene, Bmal1, regulates intestinal stem cell signaling and represses tumor initiation. Cell. Mol. Gastroenterol. Hepatol. *12*, 1847–1872.e0. https://doi.org/10.1016/j.jcmgh.2021.08.001.

25. Parasram, K., Bernardon, N., Hammoud, M., Chang, H., He, L., Perrimon, N., and Karpowicz, P. (2018). Intestinal stem cells exhibit conditional circadian clock function. Stem Cell Rep. *11*, 1287–1301. https://doi.org/10.1016/j.stemcr.2018.10.010.

26. Matsuo, T., Yamaguchi, S., Mitsui, S., Emi, A., Shimoda, F., and Okamura, H. (2003). Control mechanism of the circadian clock for timing of cell division *in vivo*. Science *302*, 255–259. https://doi.org/10.1126/science.1086271.

27. Chan, A.B., and Lamia, K.A. (2020). Cancer, hear my battle CRY. J. Pineal Res. *69*, e12658. https://doi.org/10.1111/jpi.12658.

28. Plouffe, S.W., Lin, K.C., Moore, J.L., Tan, F.E., Ma, S., Ye, Z., Qiu, Y., Ren, B., and Guan, K.L. (2018). The Hippo pathway effector proteins YAP and TAZ have both distinct and overlapping functions in the cell. J. Biol. Chem. *293*, 11230–11240. https://doi.org/10.1074/jbc.RA118.002715.

29. Oki, S., Ohta, T., Shioi, G., Hatanaka, H., Ogasawara, O., Okuda, Y., Kawaji, H., Nakaki, R., Sese, J., and Meno, C. (2018). ChIP-Atlas: a data-mining suite powered by full integration of public ChIP-seq data. EMBO Rep. *19*, e46255. https://doi.org/10.15252/embr.201846255.

30. Zhao, B., Wei, X., Li, W., Udan, R.S., Yang, Q., Kim, J., Xie, J., Ikenoue, T., Yu, J., Li, L., et al. (2007). Inactivation of YAP oncoprotein by the Hippo pathway is involved in cell contact inhibition and tissue growth control. Genes Dev. *21*, 2747–2761. https://doi.org/10.1101/gad.1602907.

31. Zhao, B., Li, L., Wang, L., Wang, C.Y., Yu, J., and Guan, K.L. (2012). Cell detachment activates the Hippo pathway via cytoskeleton reorganization to induce anoikis. Genes Dev. *26*, 54–68. https://doi.org/10.1101/gad.173435.111.

32. Zhao, B., Ye, X., Yu, J., Li, L., Li, W., Li, S., Yu, J., Lin, J.D., Wang, C.Y., Chinnaiyan, A.M., et al. (2008). TEAD mediates YAP-dependent gene induction and growth control. Genes Dev. *22*, 1962–1971. https://doi.org/10.1101/gad.1664408.

33. Li, Q., Sun, Y., Jarugumilli, G.K., Liu, S., Dang, K., Cotton, J.L., Xiol, J., Chan, P.Y., DeRan, M., Ma, L., et al. (2020). Lats1/2 sustain intestinal stem cells and Wnt activation through TEAD-dependent and independent transcription. Cell Stem Cell *26*, 675–692.e8. https://doi.org/10.1016/j.stem.2020.03.002.

34. Kang, T.H., and Leem, S.H. (2014). Modulation of ATR-mediated DNA damage checkpoint response by cryptochrome 1. Nucleic Acids Res. *42*, 4427–4434. https://doi.org/10.1093/nar/gku094.

35. Shafi, A.A., McNair, C.M., McCann, J.J., Alshalalfa, M., Shostak, A., Severson, T.M., Zhu, Y., Bergman, A., Gordon, N., Mandigo, A.C., et al. (2021). The circadian cryptochrome, CRY1, is a pro-tumorigenic factor that rhythmically modulates DNA repair. Nat. Commun. *12*, 401. https://doi.org/10.1038/s41467-020-20513-5.

36. Huang, d.W., Sherman, B.T., and Lempicki, R.A. (2009). Systematic and integrative analysis of large gene lists using DAVID bioinformatics resources. Nat. Protoc. *4*, 44–57. https://doi.org/10.1038/nprot.2008.211.

37. Zhang, B., Kirov, S., and Snoddy, J. (2005). WebGestalt: An integrated system for exploring gene sets in various biological contexts. Nucleic Acids Res. *33*, W741–W748. https://doi.org/10.1093/nar/gki475.

38. Delgado, I.L.S., Carmona, B., Nolasco, S., Santos, D., Leitão, A., and Soares, H. (2020). MOB: Pivotal conserved proteins in cytokinesis, cell architecture and tissue

homeostasis. Biology *9*, 413. https://doi.org/10.3390/biology9120413.

39. Shen, J., Cao, B., Wang, Y., Ma, C., Zeng, Z., Liu, L., Li, X., Tao, D., Gong, J., and Xie, D. (2018). Hippo component YAP promotes focal adhesion and tumour aggressiveness via transcriptionally activating THBS1/FAK signalling in breast cancer. J. Exp. Clin. Cancer Res. *37*, 175. https://doi.org/10.1186/s13046-018-0850-z.

40. Tang, Z., Li, C., Kang, B., Gao, G., Li, C., and Zhang, Z. (2017). GEPIA: A web server for cancer and normal gene expression profiling and interactive analyses. Nucleic Acids Res. *45*, W98–W102. https://doi.org/10.1093/nar/gkx247.

41. Vlug, E.J., van de Ven, R.A.H., Vermeulen, J.F., Bult, P., van Diest, P.J., and Derksen, P.W.B. (2013). Nuclear localization of the transcriptional coactivator YAP is associated with invasive lobular breast cancer. Cell. Oncol. *36*, 375–384. https://doi.org/10.1007/s13402-013-0143-7.

42. Lamia, K.A., Papp, S.J., Yu, R.T., Barish, G.D., Uhlenhaut, N.H., Jonker, J.W., Downes, M., and Evans, R.M. (2011). Cryptochromes mediate rhythmic repression of the glucocorticoid receptor. Nature *480*, 552–556. https://doi.org/10.1038/nature10700.

43. Jang, H., Lee, G.Y., Selby, C.P., Lee, G., Jeon, Y.G., Lee, J.H., Cheng, K.K.Y., Titchenell, P., Birnbaum, M.J., Xu, A., et al. (2016). SREBP1c-CRY1 signalling represses hepatic glucose production by promoting FOXO1 degradation during refeeding. Nat. Commun. *7*, 12180. https://doi.org/10.1038/ncomms12180.

44. Chiou, Y.Y., Yang, Y., Rashid, N., Ye, R., Selby, C.P., and Sancar, A. (2016). Mammalian Period represses and de-represses transcription by displacing CLOCK-BMAL1 from promoters in a Cryptochrome-dependent manner. Proc. Natl. Acad. Sci. USA *113*, E6072–E6079. https://doi.org/10.1073/pnas.1612917113.

45. Lavado, A., Park, J.Y., Paré, J., Finkelstein, D., Pan, H., Xu, B., Fan, Y., Kumar, R.P., Neale, G., Kwak, Y.D., et al. (2018). The Hippo pathway prevents YAP/TAZ-driven hypertranscription and controls neural progenitor number. Dev. Cell *47*, 576–591.e8. https://doi.org/10.1016/j.devcel.2018.09.021.

46. Yang, W.H., Ding, C.K.C., Sun, T., Rupprecht, G., Lin, C.C., Hsu, D., and Chi, J.T. (2019). The Hippo pathway effector TAZ regulates ferroptosis in renal cell carcinoma. Cell Rep. *28*, 2501–2508.e4. https://doi.org/10.1016/j.celrep.2019.07.107.

47. Strano, S., Monti, O., Pediconi, N., Baccarini, A., Fontemaggi, G., Lapi, E., Mantovani, F., Damalas, A., Citro, G., Sacchi, A., et al. (2005). The transcriptional coactivator Yes-associated protein drives p73 gene-target specificity in response to DNA Damage. Mol. Cell *18*, 447–459. https://doi.org/10.1016/j.molcel.2005.04.008.

48. Ling, J., Kang, Y., Zhao, R., Xia, Q., Lee, D.F., Chang, Z., Li, J., Peng, B., Fleming, J.B., Wang, H., et al. (2012). KrasG12D-induced IKK2/β/NF-κB activation by IL-1α and p62 feedforward loops is required for development of pancreatic ductal adenocarcinoma. Cancer Cell *21*, 105–120. https://doi.org/10.1016/j.ccr.2011.12.006.

49. Afgan, E., Baker, D., Batut, B., van den Beek, M., Bouvier, D., Cech, M., Chilton, J., Clements, D., Coraor, N., Grüning, B.A., et al. (2018). The Galaxy platform for accessible, reproducible and collaborative biomedical analyses: 2018 update. Nucleic Acids Res. *46*, W537–W544. https://doi.org/10.1093/nar/gky379.

50. Dobin, A., Davis, C.A., Schlesinger, F., Drenkow, J., Zaleski, C., Jha, S., Batut, P., Chaisson, M., and Gingeras, T.R. (2013). STAR: ultrafast universal RNA-seq aligner. Bioinformatics *29*, 15–21. https://doi.org/10.1093/bioinformatics/bts635.

51. Baker, J.M., and Boyce, F.M. (2014). High-throughput functional screening using a homemade dual-glow luciferase assay. J. Vis. Exp. https://doi.org/10.3791/50282.

STAR★METHODS

KEY RESOURCES TABLE

REAGENT or RESOURCE	SOURCE	IDENTIFIER
Antibodies		
Phospho-YAP (Ser127)	Cell Signaling Technology	#4911; RRID:AB_2218913
YAP/TAZ (D24E4)	Cell Signaling Technology	#8418; RRID:AB_10950494
LATS1 (C66B5)	Cell Signaling Technology	#3477; RRID:AB_2133513
GAPDH (D16H11) XP®	Cell Signaling Technology	#5174; RRID:AB_10622025
Horseradish secondary antibodies Rabbit	Cell Signaling Technology	#58802; RRID:AB_2799549
P21 antibody	Cell Signaling Technology	#2947S; RRID:AB_823586
p-H2AX	Cell Signaling Technology	#9718; RRID:AB_2118009
p-CHK1(S345)	Cell Signaling Technology	#2348T; RRID:AB_331212
p-CHK2(T68)	Cell Signaling Technology	#2197T; RRID:AB_2080501
CHK1	Cell Signaling Technology	#2360S; RRID:AB_2080320
CHK2	Cell Signaling Technology	#6334T; RRID:AB_11178526
vinculin	Santa Cruz Biotechnology	sc-73614; RRID:AB_1131294
b-actin	APPLIED BIOLOGICAL MATERIALS INC	#G043; RRID:AB_2631287
Cry1 antibody	Bethyl laboratories	BETHYL-A302-614; RRID:AB_10555376
Chemicals, peptides, and recombinant proteins		
TEAD Inhibitor (MGH-CP1)	synthesized in house	CAS: 896657-58-2
Dexamethasone	Sigma Aldrich	#D4902
KL001	Sigma Aldrich	#SML1032
puromycin	Gibco™	# A1113803
Critical commercial assays		
TRI reagent	Invitrogen™	#15596026
High-Capacity cDNA Reverse Transcription Kit	ThermoFisher	#4368814
PowerUp™ SYBR™ Green Master Mix	ThermoFisher	#A25776
JetPRIME transfection reagent	Polyplus transfection	#101000015
lipofectamine RNAi max	ThermoFisher	#13778075
polyethylenimine (PEI)	Polysciences, Inc.	#24765-100
Pierce™ BCA Protein Assay Kit	Thermo Scientific™	# 23225
RNeasy Mini Kit	QIAGEN	#74004
SimpleChIP® Enzymatic Chromatin IP Kit	Cell Signaling Technology	Cat #9003
Secrete-Pair™ Gaussia Luciferase kit	GeneCopoeia	# LF031
Deposited data		
RNA-seq data	Generated in house	GSE216975
Experimental models: Cell lines		
HEK293A	ATCC	# CRL-1573
MDA-MB-231	ATCC	# HTB-26
MCF7	ATCC	#HTB-22™
MCF10A	ATCC	# CRL-10317
U-2 OS	ATCC	# HTB-96™
MCF10A p-BABE	Gift from Joan S Brugge	N/A
MCF10A WT-YAP	Gift from Joan S Brugge	N/A

(*Continued on next page*)

Continued

REAGENT or RESOURCE	SOURCE	IDENTIFIER
MCF10A Mutant S127A-YAP	Gift from Joan S Brugge	N/A
HEK293 Lats1/2 ko	Gift from Wenqi Wang	N/A
HEK293 tead1/3/4 TET-ON	Gift from Junhao Mao	N/A
Oligonucleotides		
c-DNA Primers	sequence in Table S2	N/A
gDNA Primers	sequence in Table S3	N/A
Recombinant DNA		
Cry1 plasmid	Addgene	#25843
pcDNA-empty vector	Invitrogen	#V79020
WT-TAZ	Genescript	OHu14351
S89A-TAZ construct	Gift from K.-L. Guan lab (University of California, San Diego)	N/A
YAP5SA construct	Gift from K.-L. Guan lab (University of California, San Diego)	N/A
WT-YAP	Addgene	#18881
Packaging plasmid psPAX2	Addgene	#12260
Envelope plasmid VSV-G	Addgene	#14888
shRNA CRY1 (primarily)	Sigma Aldrich	TRCN0000011308
shRNA CRY1	Sigma Aldrich	TRCN0000231068
pLKO.1-YAPshRNA	Sigma Aldrich	TRCN0000095866
pLKO.1-TAZshRNA	Sigma Aldrich	TRCN0000095953
Empty sh-RNA vector	Addgene	#21915
Software and algorithms		
FastQC	Babraham Institute	https://www.bioinformatics.babraham.ac.uk/projects/fastqc
Galaxy	NIH, NSF	https://usegalaxy.org/
ImageJ	NIH	https://imagej.nih.gov/ij/
Graphpad Prism	GraphPad	https://www.graphpad.com/scientific-software/prism/

RESOURCE AVAILABILITY

Lead contact

Information and requests for resources should be directed to and be fulfilled by the Lead Contact, Xu Wu (XWU@cbrc2.mgh.harvard.edu).

Materials availability

This study did not generate new unique reagents.

Data and code availability

- This study generated new and unique RNA-seq data. The raw and processed data were deposited to gene expression omnibus under the accession number: GSE216975.
- This study did not generate new unique code.
- All data reported in this paper will be shared by the lead contact upon request. Any additional information required to reanalyze the data reported in this paper is available from the lead contact upon request.

EXPERIMENTAL MODEL AND STUDY PARTICIPANT DETAILS

Cell culture

Dulbecco's Modified Eagle Medium (DMEM), DMEM/F12 and RPMI 1640 were purchased from (Gibco), TEAD Inhibitor (MGH-CP1 synthesized in house). Dexamethasone (Sigma #D4902). CRY activator KL001 (Sigma #SML1032).

HEK293A and MDA-MB-231 cells (ATCC, Cat# CRL-1573, Cat# HTB-26) were grown in DMEM, and MCF7 (ATCC, Cat#HTB-22™), cells were grown in RPMI1640. Culture media were supplemented with 10% fetal bovine serum (FBS), 100 U/mL penicillin, and 100 U/mL streptomycin. MCF10A (ATCC, Cat# CRL-10317) cells were grown in DMEM/F12 supplemented with (5% Horse serum, 20 ng/mL EGF, 0.5 μg/mL hydrocortisone, 100 ng/ml cholera toxin, 10μg/mL insulin and 100 U/mL penicillin/streptomycin). Cells between three and ten passages were used for experiments. Cultures were maintained at 37°C in a humidified 5% CO_2 incubator. The concentration and duration of the inhibitors used are described in figure legends. Equivalent volume of solvent (DMSO) was used as a control.

METHOD DETAILS

Quantitative real-time PCR

Cells were directly resuspended in TRI reagent (#15596026, Invitrogen™). Total RNAs were then isolated following manufacturers' instruction. Purified RNAs were dissolved in nuclease-free water. cDNA was generated from 1 μg RNA using High-Capacity cDNA Reverse Transcription Kit (ThermoFisher, #4368814). Mixtures containing 30 ng cDNA, 30μL PowerUp™ SYBR™ Green Master Mix (ThermoFisher, #A25776) and 300 nM forward and reverse primers were run in duplicates on QuantStudio™ 5 Real-Time PCR System. q-PCR conditions were as follows, first 2 min polymerase activation at 95°C then 40 cycles at 95°C for 30 s and 61°C for 30 s and 72°C for 30s. Melting curve analysis of the PCR was then performed to verify primer specificity. For quantification, Gapdh was used as housekeeping genes. Primer sequences are shown in Table S2.

Transient transfection

HEK293A Cells were plated in six-well plates 24 h before transfection at 60% confluence. JetPRIME transfection reagent (Polyplus transfection) was used to transfect expression constructs into cells. First, two μg of each plasmid and 4μg of PEI were separately diluted in 150 μL of Opti-MEM (Gibco™). Five minutes later, the two mixtures were combined and vortexed. Twenty minutes later the mixture was added dropwise to each well. Twenty-four hours later medium was replaced then cells were treated as indicated. Both RNA and protein analyses were performed 48 h after transfection. For siRNA transfection, lipofectamine RNAi max was used following manufacturer's instruction (ThermoFisher # 13778075). The following siRNA were used (siRNA control (Sigma, #SIC001), the siRNA sequences used in silencing YAP/TAZ experiments were: GACAUCUUCUGGUCAGAGA dTdT (YAP), ACGUUGACUUAGGAACUUU dTdT (TAZ). The following plasmids were used for transient transfection Cry1 (Addgene, Cat #25843), pcDNA-empty vector (Invitrogen), WT-TAZ (Genescript, OHu14351), S89A-TAZ (K.-L. Guan lab), WT-YAP (Addgene, #18881), YAP5SA (K.-L. Guan lab).

Packaging shRNA-Encoding Lentivirus

HEK293T cells were plated in a 10 cm culture dish a day before at 50% confluency. Sixteen hours later, the medium was replaced. The following mixtures were separately prepared. Packaging plasmid (psPAX2, 2.6μg), Envelope plasmid (VSV-G, 0.875μg) and 3.5μg of each sh-RNA plasmid were diluted in 500 μL of Opti-MEM. 14ug polyethylenimine (PEI) was diluted in 500 μL of Opti-MEM. 5 min later, the two mixtures were combined and vortexed. After 20 min incubation at RT, the mixture was added dropwise to each plate. Six hours later, the medium was replaced. Lentiviral supernatants were then collected 24 and 48 h later and filtered using a 0.45 μm syringe filter to remove cell debris. Lentiviral supernatants were then stored at −80°C until further use. The following shRNA were used CRY1 (primarily TRCN0000011308, and TRCN0000231068, Sigma), YAP (pLKO.1-YAPshRNA, TRCN0000095866), and TAZ (pLKO.1-TAZshRNA, TRCN0000095953). Empty vector was used as a control (Addgene, Cat #21915).

Lentivirus infection and selection

Cells were plated in six-well plates a day before at 60% confluence. Sixteen hours later the medium was changed to 2 mL medium containing 1 mL complete medium and 1 mL of lentiviral supernatant. To increase

the efficiency of lentiviral infection, medium was supplemented with 10μg/mL polybrene. Sixteen hours later, the medium was replaced. Selection with 2 μg/mL puromycin (Gibco™, # A1113803) was performed 72 h post-infection for 4 days to eliminate the non-infected cells. Knockdown efficiently was verified using qPCR and western blot.

Western blotting

Upon the indicated treatment, cells were washed with PBS then resuspended in lysis buffer containing 50 mM Tris-HCl, pH 8.0, 150 mM NaCl, 0.5% sodium deoxycholate, 1.0% NP-40, 0.1% SDS, and protease/phosphatase inhibitors (Roche #11836153001, #4906845001). Total extracts were incubated for 10 min on ice, then centrifuged for 10 min. Protein concentrations were quantified using Pierce™ BCA Protein Assay Kit (Thermo Scientific™ # 23225), according to the manufacturer's instructions. Proteins were then separated by SDS-PAGE and transferred to the Polyvinylidene fluoride (PVDF) membrane. Membranes were blocked with tris-buffered saline containing 0.05% Tween 20 and 5% non-fat milk. The following antibodies were all purchased from cell signaling (Phospho-YAP (Ser127) #4911, YAP/TAZ (D24E4) mAb #8418, LATS1 (C66B5) Rabbit mAb #3477, GAPDH (D16H11) XP® Rabbit mAb #5174, Horseradish secondary antibodies Rabbit #58802. Cry1 antibody was purchased from Bethyl laboratories (BETHYL-A302-614). Catalog ID of the following antibodies P21 (Cell Signaling Technology, #2947S), p-H2AX (Cell Signaling Technology, #9718), p-CHK1(S345) (Cell Signaling Technology, #2348T), p-CHK2(T68) (Cell Signaling Technology, #2197T), CHK1 (Cell Signaling Technology, #2360S), CHK2 (Cell Signaling Technology, #6334T), vinculin (Santa Cruz, #sc-73614) and b-actin (APPLIED BIOLOGICAL MATERIALS INC, #G043). Antibody dilutions were prepared according to the manufacturer's instructions.

RNA-seq data analysis

For sequencing analysis, two independent biological replicates of cells were collected for each condition. Total RNA was isolated using TRI reagent then purified with Rneasy Mini Kit (QIAGEN#74004). Quality control, library preparation, and sequencing was performed by Novogene. Briefly, RNA quality was verified using agarose gel electrophoresis and Agilent 2100. Oligo(dT) beads were used to enrich mRNA, and rRNA were removed using the Ribo-Zero kit. After fragmentation, total cDNA was synthesized using random hexamers primer followed by cDNA second-strand synthesis. After a series of terminal double-stranded cDNA libraries are completed through size selection and PCR enrichment. Later quality control cDNA libraries were submitted to paired-end sequencing (PE150).

The following low-quality reads and adapters were filtered at Novogene. Reads containing adapters, reads with N > 10% and reads with low quality (Qscore<= 5) base, which is over 50% of the total base. Sequence quality was further verified using FastQC (https://www.bioinformatics.babraham.ac.uk/projects/fastqc/). RNA seq data analysis was then performed using the galaxy pipeline, applying the default parameters of each program.[49] Raw reads were aligned using STAR[50] to the human genome version (hg38). Transcriptome quantification was performed using feature Counts.

Differential expression was performed using edgeR, using the TMM normalization method. Benjamini-Hochberg correction was used to correct for multiple comparisons (with a false discovery cut-off <0.05). Genes below this threshold are considered significant. Functional analysis was performed using DAVID (the database for annotation, visualization, and integrated discovery).[36] This analysis was performed only on the list of differentially expressed genes. Gene set enrichment analysis was performed to confirm DAVID results using WebGestalt.[37] RNA-seq raw and processed data were submitted to gene expression omnibus under the accession numbers GSE216975.

Colony forming assay

Equal number of cells stably transfected with shRNA control or shRNA against CRY1 were plated into 24-well plates containing 1 mL of culture medium (1000 cells/mL). Cells were then grown for 14 days at 37°C and 5% CO_2. Cell colonies were fixed with ice-cold methanol and then stained with crystal violet. The content was solubilized using 10% acetic acid to measure the crystal violet in each well. The absorbance of the solution was measured on VICTOR Multilabel plate reader (PerkinElmer) at a wavelength of 590 nm.

Chromatin immunoprecipitation assay

ChIP was performed as described in the protocol supplied with the kit from cell signaling technology (Cat #9003) with some modifications. Briefly, HEK293A cells transfected with the indicated constructs were first cross-linked with 1% formaldehyde for 10 min at room temperature. After quenching of formaldehyde with 125 mM glycine, cells were directly resuspended in 1X ChIP buffer then chromatin was sheared by sonication. As analyzed on agarose gels, the fragmented chromatin was around 300–1200 bp. Chromatin (500 μg) from each condition was subjected to immunoprecipitation with the indicated antibodies at 4°C overnight. Immune-complexes were recovered by incubation with protein G beads for 2 h at 4°C. DNA was purified using the reagents supplied in the kit. The primers used for qPCR can be found in Table S3.

Luciferase reporter assay

The expression vectors used were from the following sources: Cry1 transcription luciferase reporter (Addgene #110056). pEZX-PG02-YAP-Luc was purchased from GeneCopoeia (#HPRM34974-PG02). The promoter sequence of human YAP was cloned to the upstream of firefly luciferase gene in the pEZX-PG02 vector. Upon transfection with the indicated plasmid, cells were left to grow for 48 h. CRY1 reporter activity was measured using the homemade dual-glow luciferase assay protocol previously described.[51] Briefly, the CRY1 reporter was transfected together with p-CDNA-YAP and Renilla luciferase constructs into HEK293A cells. 24 h later, cell lysates were prepared using 25mM Tris-phosphate pH 7.8, 2mM DTT, 2mM 1,2-diaminocyclohexane- N,N,N′,N′-tetra acetic acid, 10% glycerol and 1% Triton® X-100. Substrate for firefly luciferase containing 25mM Tris-phosphate pH 7.8,1mM luciferin, 3mM ATP, 15mM $MgCl_2$, 0.2mM CoEnzyme A, and 1M DTT were then added. Renilla luciferase activity was measured using the following substrate buffer containing 0.01mM h-CTZ and 0.06mM PTC124, 45mM Na_2EDTA, 30mM Pyrophosphate tetrabasic, and 1.425M NaCl. Luminescence of Firefly and Renilla luciferase activities were then measured using VICTOR Multilabel plate reader (PerkinElmer). YAP-promoter activity was measured using the Secrete-Pair™ Gaussia Luciferase kit according to the manufacturer's instructions (GeneCopoeia# LF031).

QUANTIFICATION AND STATISTICAL ANALYSIS

Statistical tests were performed using GraphPad Prism (http://www.graphpad.com). All experiments were performed in triplicate. One-way ANOVA with Tukey post hoc test was applied to compare the means of three or more groups. Unpaired, two-sided Student t tests were used to compare the means of two groups. Results are expressed as means ± SEM. $P < 0.05$ was considered to be significant. The statistical analyses of the data are shown in Table S4.